A GLOBAL ASSESSMENT OF TSUNAMI HAZARDS OVER THE LAST 400 YEARS

WORLD TSUNAMI AWARENESS DAY
5 NOVEMBER 2016

TOHOKU UNIVERSITY

IRIDeS
International Research Institute of Disaster Science
災害科学国際研究所

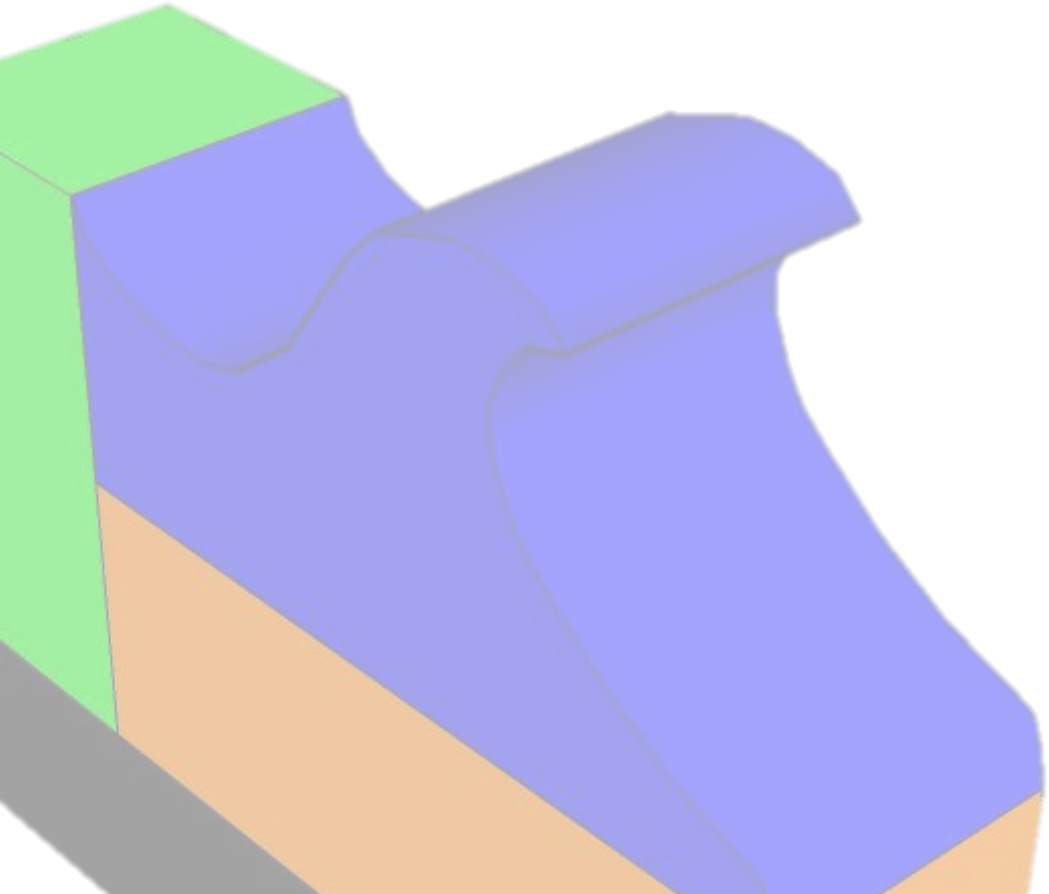

Contributors:

Japan Asia Group
KOKUSAI KOGYO

esri Japan

TOKIO MARINE NICHIDO

Willis Research Network

A GLOBAL ASSESSMENT OF TSUNAMI HAZARDS OVER THE LAST 400 YEARS

Prepared by
Fumihiko Imamura
Anawat Suppasri
Panon Latcharote
Takuro Otake

International Research Institute of Disaster Science (IRIDeS)
Tohoku University

Contributors:
Kokusaikogyo Co., Ltd.,
Esri Japan Corporation,
Tokio Marine & Nichido Fire Insurance Co., Ltd., and
Willis Research Network

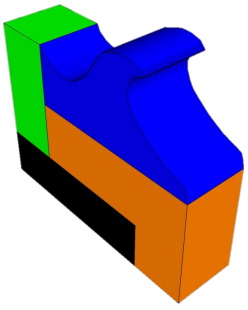

Updated on 27 December 2016
First published on 31 October 2016

Executive Summary

This report is our contribution towards World Tsunami Awareness Day, which was proposed by the United Nations (UN) in 2015. We conducted a global tsunami hazard assessment for local regions, including low tsunami risk areas, based on a 400-year database which allows insight on potential future tsunamis based on the seismic gap.

The resulting tsunami hazard could be displayed on a global map and enable us to easily observe the local effects of tsunamis. Two criterions were selected to represent the past 100 major earthquake generated tsunamis: first, the earthquakes must be larger than magnitude 7.5 and secondly, occurred after the year 1600. Based on the results of the simulation, the locations of modern tsunamis (from the periods of 1970 to 2016) greater than 2 meters in height, are limited to areas affected by the 2004 Indian Ocean Tsunami, and the 2011 Great East Japan Tsunami. Regardless, damaging tsunamis have been witnessed everywhere in the world, especially along the Pacific Rim. This observation shows the importance of assessing or knowing the hazards based on historical events beyond our memory. Comparisons between tsunami height and wave force show that only using the tsunami height might underestimate the building damage. We wish that as a part of the World Tsunami Awareness Day related activities, our results and findings will increase tsunami awareness at the global scale, especially in comparatively low tsunami risk areas, and reduce human loss from future tsunamis.

1. Purpose

A tsunami is classified as a low-frequency and high-impact natural hazard. Reducing tsunami vulnerabilities, managing risks, and limiting its effects based on global-scale scientific assessments can be difficult due to the lack of information and experience. While high tsunami risk regions such as the Pacific and Indian Oceans have implemented countermeasures based on lessons and experiences from the past, much fewer measures have been adopted in low-risk areas. In such cases, although the risk of a tsunami is less likely than high risk areas, unknown risks continue to persist and the potential for even small tsunamis to cause catastrophic damages exist. Once a tsunami is generated from a seismic fault or landslide, the wave can propagate across entire oceans and affect many countries (*United Nations International Strategy for Disaster Reduction (UNISDR), 2009; Løvholt et. al, 2012*). This phenomenon is why international collaboration with networks for tsunami mitigation is essential. We can properly evacuate people and save lives by using the available time before a tsunami arrives after its initial propagation across an ocean., In other words, knowledge and information can save lives from the threat of tsunamis, including the possibility of achieving zero human losses with proper preparation.

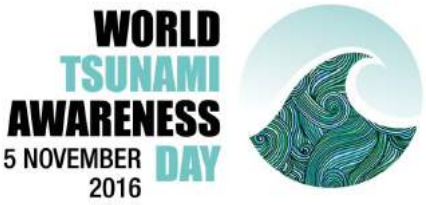

We wish to contribute to **World Tsunami Awareness Day**, which was proposed by the UN in 2015, by conducting a global tsunami hazard assessment for local regions based on a 400 year data base which can allow stakeholders to anticipate future tsunamis based on seismic gaps. The resulting tsunami hazard data can be displayed on a global map that will easily enable users to observe the local effects of tsunamis.

2. Major Earthquake-Generated Tsunami in the Last 400 Years

Within a roughly 10 year period between the 1950s to 1960s, three devastating tsunamis were generated by earthquakes that were magnitude (M_w) 9.0 or larger (*Tsunami Laboratory, 2016*). All of them were located along the Pacific Rim. The 1952 Kamchaka earthquake (9.0 M_w) generated large tsunamis that caused catastrophic damages and human loss around the Kamchatka Peninsula and the Kuril Islands, while Hawaii received property damages but no human casualties, and no damages and casualties in Japan (*Johnson & Satake, 1999*). The 1960 Chilean Tsunami was generated by a (9.5 M_w) (9.5 M_w) earthquake, the largest ever instrumentally recorded, causing widesperad damage and human loss due to the accompanying transoceanic tsunami that also impacted Hawaii and Japan (*Fujii & Satake, 2013*). The 1964 Alaskan Earthquake (9.2 M_w) is the second largest observed Earthquake (*Ichinone et al., 2007*). Its associated tsunami hit a large part of southern Alaska and neighboring areas of the western Canada and the West Coast of US but with minor damage and no fatalities in Hawaii. After the end of this series of devastated tsunamis that was noticed all over the world, other major tsunamis such as the 2011 Great East Japan tsunami were occurred along the Pacific Rim excepted the 2004 Indian Ocean tsunami.

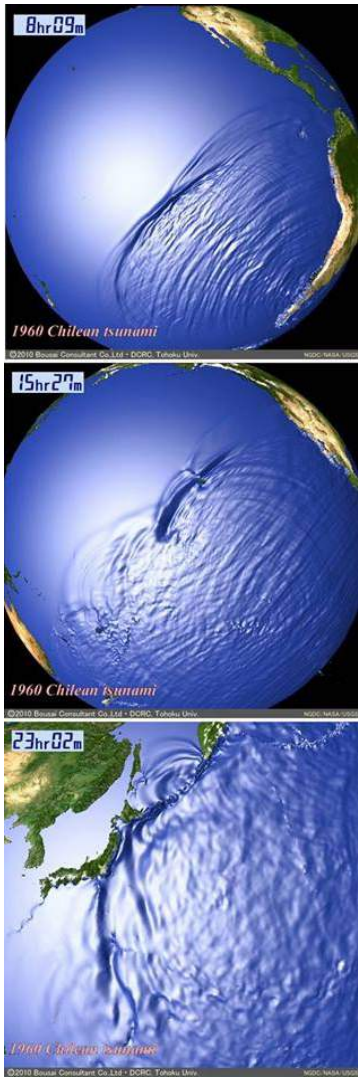

Figure 1

Simulation of the 1960 Chilean tsunami

Although the Pacific Ocean is considered the most tsunami risk region, information on historical tsunamis exist in even low tsunami risk areas such as the Atlantic Ocean, the Mediterranean Sea, the Black Sea, the Caribbean Sea and the western United States. For example , the 1700 Cascadia earthquake occurred along the west coast of the US with the estimated magnitude of 9.0 M_w. A Large transoceanic tsunami followed the earthquake and struck the west coast of the US and Canada. The tsunami also hit the coast of Japan based on Japanese records, noting that the wave was not tied to any other Pacific Rim earthquake. Within Europe, the 1755 Lisbon Tsunami was one of the most catastrophic events that had ever occurred in Atlantic Ocean and devastated Europe, particularly in modern-day Portugal, Spain and Morocco, with waves observed in Ireland and the Lesser Antilles (*Santos et al., 2009*).

The tsunami caused severe damages and large number of casualties as high as 60,000. (*Tsunami Alarm System, 2016a*). In the Mediterranean Sea, it is said that one disastrous tsunami takes place in this region on average, every century, based on a long record of historical tsunamis since 1628 BC (*Tsunami Alarm System, 2016b*). Greece, Turkey and southern Italy are the most tsunami affected countries in the region. There are some major tsunamis such as local tsunamis that damaged southern Italy in 1905 and 1907, another tsunami that affected Cyclades and Dodecanese Islands, Crete, and the Turkish coast of Asia Minor. In 1956 (*Okal et al., 2009*), and a local tsunami within the enclosed Sea of Marmara in 1999 (*Latcharote et al., 2016*) led to an estimated 17,000 fatalities (*Tsunami Alarm System, 2016b; Piatanesi & Tinti, 2002*).

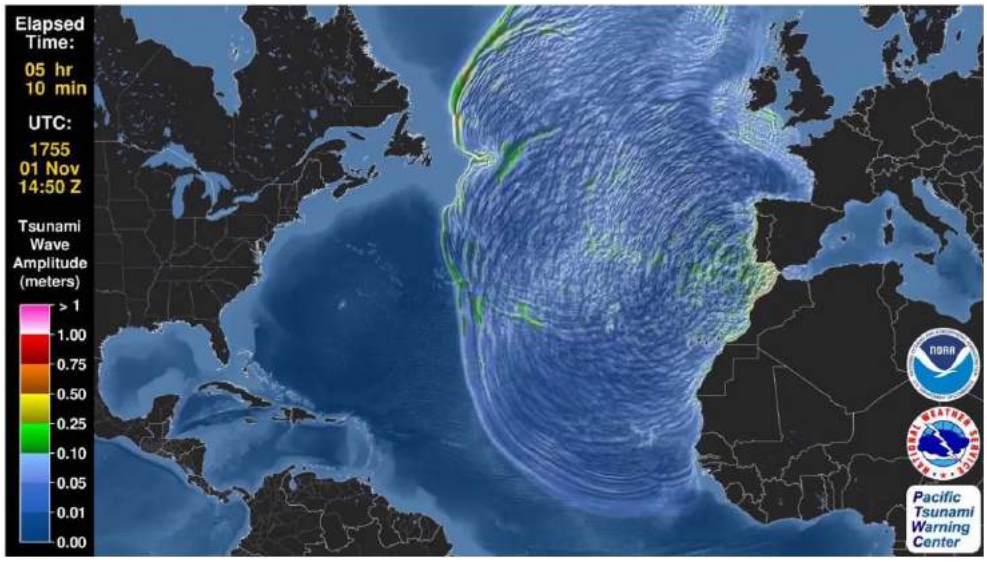

Figure 2

Simulation of the 1755 Lisbon tsunami

***Note*. Source: *Tsunami forecast model animation of 1 November 1755 Lisbon, Portugal tsunami*, by D. Wang, & N. Becker, 2015.**

3. Selection of Seismic Events

100 major historical earthquake-generated tsunamis were selected to represent tsunami hazards on a global scale. These 100 events were selected from a total of 17 tsunami source regions from a global historical tsunami database (*National Geophysical Data Center/World Data Service (NGDC/WDS), 2016*). Two main criteria were used for the event selection.

First, the earthquake magnitude must be larger than 7.5, which is the general condition for earthquake-induced tsunamis. Since the first criteria relies on the magnitude of the earthquake regardless of fault mechanism, some events exist where a large magnitude earthquake occurred but generated a small tsunami due to a strike-slip fault mechanism.

In addition, seismic events that produced landslides occurred, however most of the fault parameters only represent seismic sources. Only the 1771 Meiwa Tsunami which had a landslide source, was represented as a seismic source for the sake of convenience.

Secondly seismic events after 1600 were selected due to the return period of large earthquakes is generally greater than 300-400 years. Seismic gap regions will be considered in future research.

Seismic Gap
A seismic gap as defined by the U.S. Geological Survey (*USGS, 2016*) is a section of a fault that has produced earthquakes in the past but is now quiet.

For some seismic gaps, no earthquakes have been observed historically, but it is believed that the fault segment is capable of producing earthquakes on some other basis, such as plate-motion information or strain measurements.

4. List of Earthquake Events and Its Distributions

Table 1 List of earthquake induced tsunami events

No.	Year	M	Location	Lat.	Lon.	Max. Water Height (m)	Deaths	Damage ($Mill.)	House Destroyed
1	1677	8.0	Boso	35.000	142.000				
2	1687	8.5	S Peru	-13.500	-76.500		5,000		
3	1692	7.7	Jamaica	17.800	-76.700	1.8	2,000		
4	1700	9.0	Cascadia Subduction Zone	45.000	-125.000		2		
5	1703	8.2	Off SW Boso Peninsula	34.700	139.800	10.5	5,233		20,162
6	1707	8.4	Nankaido	33.200	134.800	25.7	5,000		17,000
7	1730	8.7	Central Chile	-32.500	-71.500				
8	1755	8.5	Lisbon (Portugal)	37.000	-10.000	18.3	50,000		
9	1762	8.8	Arakan	21.000	89.000	1.8			
10	1771	7.5	Ishigaki Is. (Meiwa)	24.000	124.600				
11	1787	8.3	San Marcos	16.500	-98.500	4.0	11		
12	1788	8.0	Alaskan Peninsula	57.000	-153.000	30.0			
13	1812	7.5	S California	34.200	-119.900	3.4			
14	1833	8.3	SW Sumatra	-2.500	100.500				
15	1837	8.5	S Chile	-42.500	-74.000	6.0	16		
16	1842	8.1	Haiti	19.750	-72.200	5.0	300		
17	1843	8.3	Guadeloupe (French Territory)	16.500	-62.200	1.2			
18	1852	8.3	Banda Sea	-5.250	129.750	8.0	60		
19	1854	8.3	Enshunada Sea	34.000	137.900	21.0	300		8,300
20	1865	8.0	Tonga Is.	-19.500	-173.500	1.3			20
21	1868	7.9	Hawaii	19.000	-155.500	13.7	47		108
22	1868	8.5	S Peru	-18.600	-71.000	18	25,000		
23	1877	8.3	N .Chile	-21.500	-70.500	24.0	2,282		

No.	Year	M	Location	Lat.	Lon.	Max. Water Height (m)	Deaths	Damage ($Mill.)	House Destroyed
24	1882	7.9	Panama	10.000	-79.000	3.0			
25	1886	7.7	Charleston (USA)	32.900	-80.000				
26	1889	8.0	N Moluccas Is.	1.000	126.250	4.0			
27	1897	8.7	Sulu Sea	6.000	122.000	7.0	13		33
28	1899	8.2	Yakutat Bay	60.000	-140.000	61.0			
29	1905	7.9	Italy	39.000	16.000	1.3			
30	1906	8.8	Off Coastal Ecuador	1.000	-81.500	5.0	1,000		
31	1917	8.0	Kermadec Is.	-29.200	-177.000	0.3			
32	1917	8.3	Samoa Is.	-15.500	-173.000	12.2			
33	1918	8.3	Celebes Sea	5.500	123.000	7.2	6		
34	1918	8.2	S Kuril Is.	45.500	151.500	12.0			
35	1919	8.1	Tonga Is.	-18.352	-172.515	2.5	23		2
36	1922	8.7	N Chile	-28.553	-70.755	9.0	200		
37	1924	8.3	E Mindanao Is.	6.500	126.500				
38	1932	8.1	Central Mexico	19.500	-104.300	10.0	4		
39	1933	8.4	Sanriku	39.224	144.622	29.0	3,022		6,000
40	1934	7.9	South China Sea	17.500	119.000				
41	1938	8.5	Banda Sea	-5.250	130.500	3.4			
42	1939	7.7	S Black Sea (Turkey)	39.770	39.533	0.5			
43	1941	8.3	Azores Gibraltar Fracture Zone	37.417	-18.983	0.1			
44	1941	7.6	Andaman Sea, E Coast of India	12.500	92.500	1.5			
45	1945	8.0	Makran Coast	24.500	63.000	17.0	4,000	25	
46	1946	8.6	Aleutian	53.492	-162.832	42.0	167	24	
47	1948	8.3	Sulu Sea	10.500	122.000	67.1	124	116	
48	1948	7.8	Tonga Trench	-21.000	-174.000	2.0			
49	1949	8.1	British Columbia	53.600	-133.300	0.6			
50	1952	8.1	Tokachi	42.150	143.850	6.5	33		
51	1952	9.0	Kamchatka	52.755	160.057	18.4	10,000	1	
52	1956	7.8	Greece	36.900	26.000	30.0	3		
53	1960	9.5	S Chile	-38.143	-73.407	25.0	2,223	1,000	58,622
54	1964	9.2	Alaska	61.017	-147.648				

No.	Year	M	Location	Lat.	Lon.	Max. Water Height (m)	Deaths	Damage ($Mill.)	House Destroyed
55	1964	7.5	NW .Honshu Is.	38.650	139.200	5.8	26	80	1,960
56	1965	8.7	Rat Is. aAnd Aleutian Is.	51.300	178.600	10.7		0.1	
57	1965	7.8	Mexico	16.300	-95.800	0.4			
58	1969	7.7	Kamchatka	57.700	163.600	15.0			
59	1973	7.5	Quezon (Philippines)	13.400	122.800	1.3			
60	1975	7.6	Philippine Trench	12.540	125.993	3.0			30
61	1975	7.9	Solomon Sea	-6.590	155.054	2.0			
62	1976	8.0	Moro Gulf	6.292	124.090	9.0	6,800	134	
63	1977	8.0	Sunda Is.	-11.085	118.464	15.0	189	1	
64	1977	8.1	Solomon Is.	-9.965	160.731	0.04			
65	1980	7.7	Algeria	36.195	1.354	0.7			
66	1983	7.8	Noshiro	40.462	139.102	14.9	100	800	3,513
67	1985	8.0	Mexico	18.190	-102.533	3.0			
68	1986	7.8	Taiwan	23.901	121.574	0.3			
69	1990	7.5	Mariana Trench, N Mariana Is.	15.125	147.596	1.8			
70	1992	7.8	Flores Sea	-8.480	121.896	26.2	1,169	100	31,785
71	1992	7.7	Nicaragua	11.727	-87.386	9.9	170	30	1,500
72	1993	7.7	Sea of Japan	42.851	139.197	32.0	208	1,207	2,374
73	1994	8.3	S Kuril Is.	43.773	147.321	10.4			2
74	1996	7.9	Sulawesi	0.729	119.931	7.7	9	1	400
75	1996	8.2	Irian Jaya	-0.891	136.952		110	4	
76	1996	7.5	N Peru	-9.593	-79.587	5.1	12		15
77	1997	7.7	Santa Cruz Is., Vanuatu	-12.584	166.676	3.0			7
78	1997	7.8	Kamchatka	54.841	162.035	8.0			
79	1999	7.6	Turkey	40.760	29.970	2.5	155		
80	1999	7.5	Vanuatu Is.	-16.423	168.214	6.6	5		
81	2000	7.6	Sulawesi	-1.105	123.573	6.0			
82	2000	8.0	New Ireland	-3.980	152.169	3.0			
83	2001	8.4	S Peru	-16.265	-73.641	8.8	26		2,000
84	2002	7.6	Bismarck Sea	-3.302	142.945	5.5			
85	2004	9.1	Off W .Coast of Sumatra	3.316	95.854	50.9	227,899	10,000	

No.	Year	M	Location	Lat.	Lon.	Max. Water Height (m)	Deaths	Damage ($Mill.)	House Destroyed
86	2004	8.1	Macquarie Is.	-49.312	161.345	0.3			
87	2005	8.7	Nias	2.085	97.108	4.2	10		
88	2006	7.7	S Java	-9.254	107.411	20.9	802	55	1,623
89	2006	8.3	S Kuril Is.	46.592	153.266	21.9			
90	2007	8.1	Solomon Is.	-8.460	157.044	12.1	52		2,500
91	2010	8.8	Central Chile	-36.122	-72.898	29.0	156	30,000	
92	2011	9.0	Honshu Is.	38.297	142.372	38.9	18,453	220,085	273,796
93	2013	7.9	Santa Cruz Is.	-10.766	165.114	12.1	52		2,500
94	2013	7.8	Scotia Sea (Antarctica)	-60.296	-46.362	0.2			

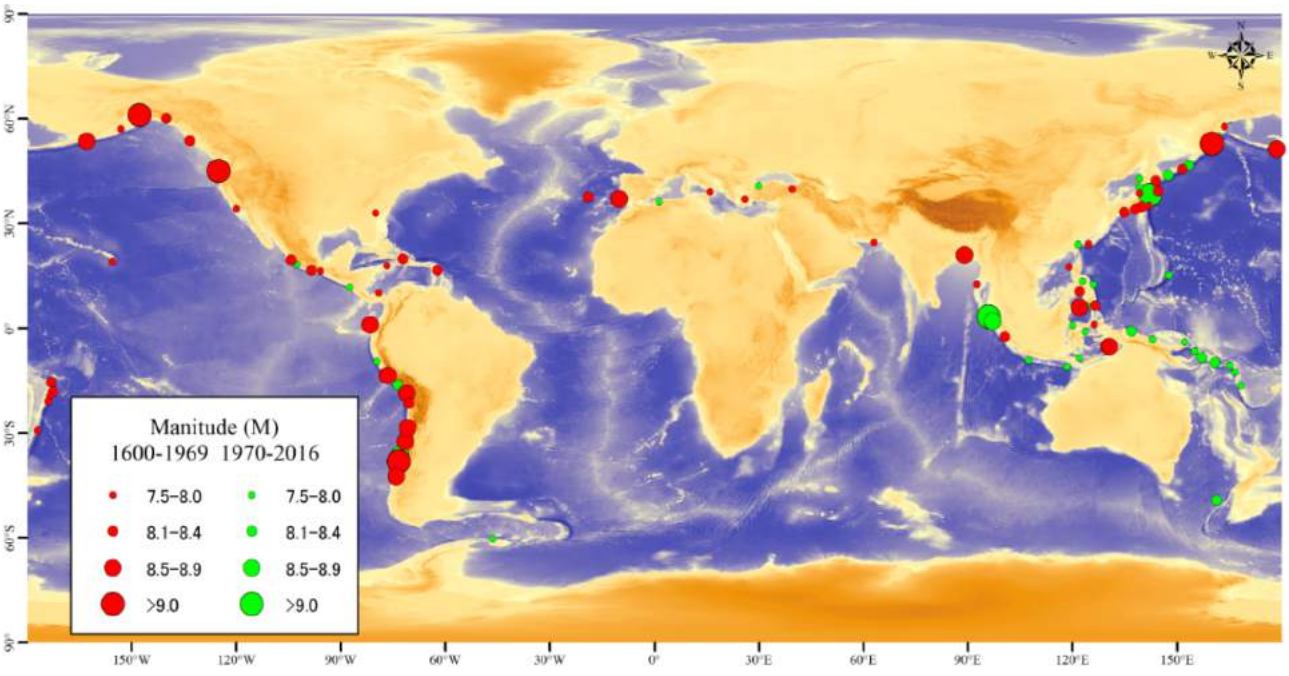

Figure 3

Distributions of the 94 selected earthquakes

***Note*. Green: 36 events that occurred during 1970 to 2016;**
Red: 58 events that occurred during 1600-1969.
The sizes of the circles indicate the earthquake magnitude, which ranges from 7.5 to greater than 9.0 and greater.

5. Earthquake Fault Parameters

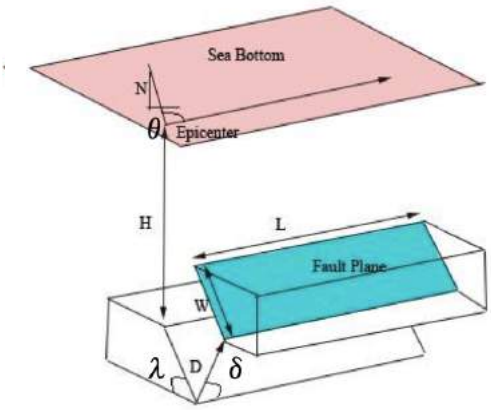

Figure 4

Illustration of earthquake fault parameters

Source: *Tsunami Modelling Manual (TUNAMI model)*, by F. Imamura, A. C. Yalciner, & G. Ozyurt, 2006, p. 15.

Only static fault parameters (rupture velocity was considered to be infinite) were used to calculate seafloor and coastal deformation. Nine fault parameters were required for each earthquake event, namely, the latitude, longitude, focal depth (H), fault length (L), fault width (W), displacement (D), strike angle (θ), dip angle (λ) and rake angle (δ).

Generally, the aforementioned fault parameters were primarily selected from previously published literature for each earthquake event. Missing fault mechanism information (strike, dip and slip angles) was obtained from other nearby events that were listed in the Global Centroid Moment Tensor (CMT) catalog since 1976 (*Dziewonski et al., 1981*). The scaling law that was proposed by *Papazachos et al. (2004)* was applied for events with missing fault geometry information (length, width and displacement). Examples of subduction zone fault parameters are as follows:

Fault length, L (in km):	**$\log L = 0.55\ Mw - 2.19,\ 6.7 \leq Mw \leq 9.2$**	**(1)**
Fault width, W (in km):	**$\log W = 0.31\ Mw - 0.63,\ 6.7 \leq Mw \leq 9.2$**	**(2)**
Displacement, D (in cm):	**$\log D = 0.64\ Mw - 2.78,\ 6.7 \leq Mw \leq 9.2$**	**(3)**

6. Bathymetry and Topography Data

Two main computational regions exist regarding the energy distribution of each tsunami event, namely, the bathymetry and topography, which are focused within 1) the Pacific and Indian Oceans and 2) the Atlantic Ocean.

6.1 The Pacific Ocean and Indian Ocean

Column (x): 4,320
Row (y): 2,160
Cell size: 0.083333333
(5 arc-min, about 10 km)
xllcorner: -25 and yllcorner: -90

A General Bathymetric Chart of the Oceans (GEBCO) 30 arc-sec (approximately 900 m) grid (*GEBCO, 2016*) was used as the original bathymetry and topography data for the simulation. The data was then resampled to a resolution of 10 km (5 arc-min) to conduct numerical tsunami simulations on a global scale.

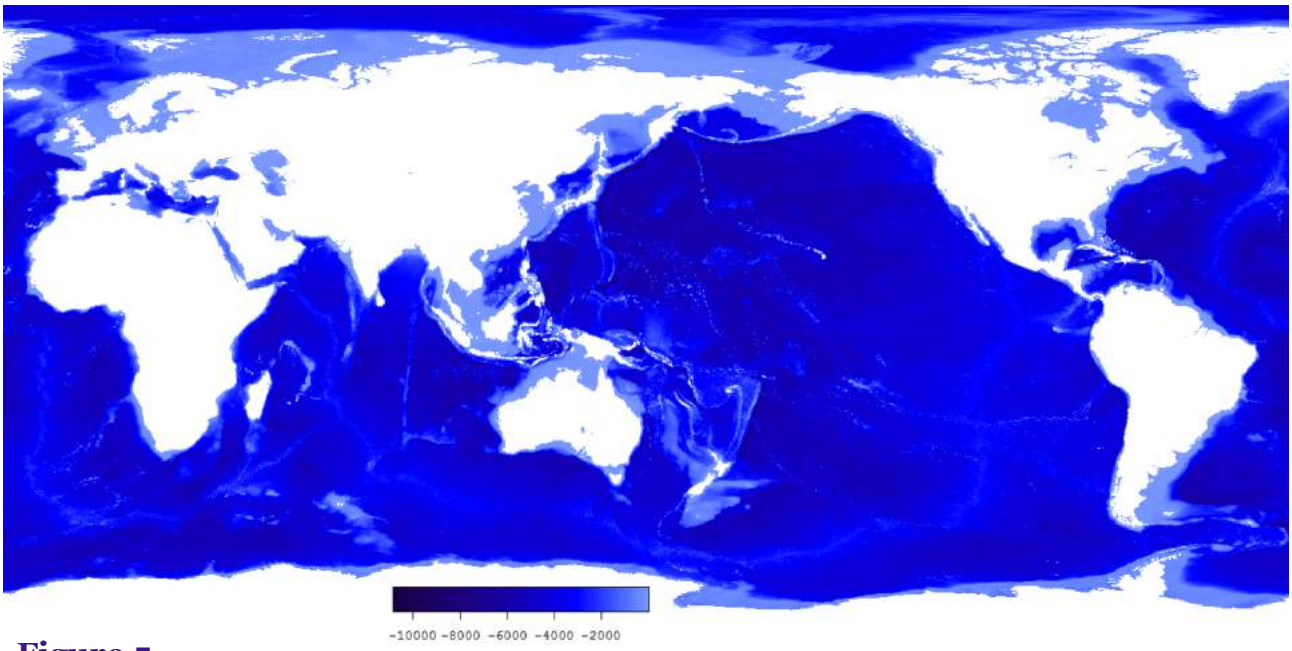

Figure 5

Bathymetry and topographic data from the Pacific Ocean and Indian Ocean

6.2 Atlantic Ocean

Column (x): 3,240
Row (y): 1,728
Cell size: 0.083333333
(5 arc-min, about 10 km)
xllcorner: -135 and yllcorner: -72

Bathymetry and topography data from the Atlantic Ocean were utilized in order to better understand seismic events that caused transoceanic tsunamis across the Atlantic Ocean, particularly those that affected Europe, the eastern coast of the United States, and the Caribbean Sea.

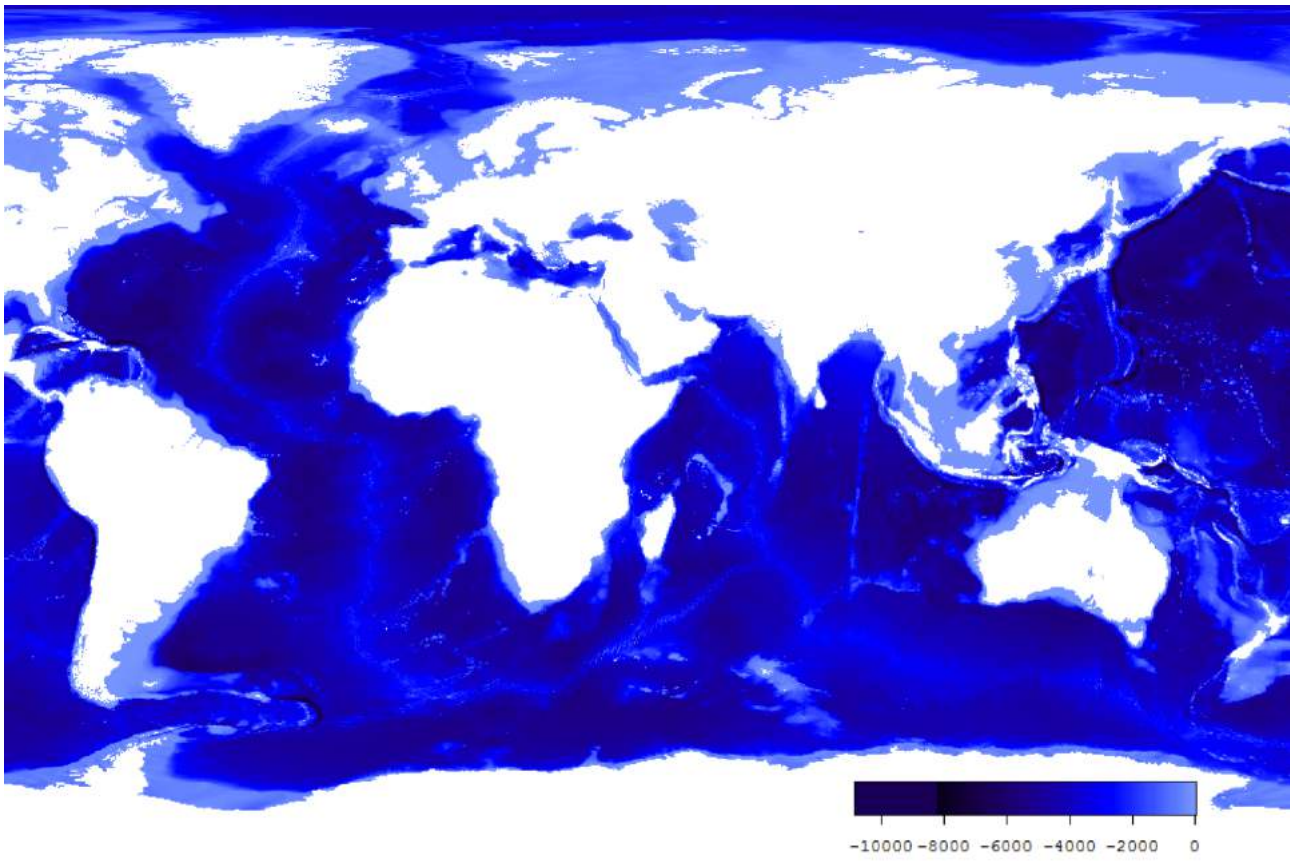

Figure 6

Bathymetry and topographic data from the Atlantic Ocean

7. Tsunami Numerical Simulation

Numerical simulations of distant source tsunamis were conducted by using a code that was developed by Tohoku University, namely, the **Tohoku University's Numerical Analysis Model for the Investigation of Near–field tsunamis (TUNAMI)** (*IUGG/IOC TIME Project, 1997*). This model uses a staggered leap-frog scheme to solve shallow water equations that describe the nonlinear long-wave theory (*Imamura, 1996; Nagano et al., 1991; Suppasri et al., 2010*). These simulations were performed following the fault parameters for each case, as previously shown in Table 1. The initial sea surface conditions were prepared by using formulas to calculate seafloor and coastal deformation from submarine faulting with earthquake fault parameters (Okada, 1985). The simulation time was set to 24 h, ensuring that the maximum tsunami height would be obtained and that the tsunami could travel across the oceans. A reflective boundary condition was imposed on the shorelines across the entire area to ignore tsunami inundation along the coast. Therefore, wave amplification in nearshore areas was not considered in these simulations.

Q: What is the earliest possible warning that one can receive before a tsunami hits the shore?

A: Shaking due to a large earthquake can range from one to three minutes and can be considered as a prelude to a tsunami. For distant locations where the shaking could not be felt, national level tsunami warning systems can be disseminated within 3 minutes in Japan (*Suppasri et al., 2016*), about 7 minutes in Thailand, (*Leelawat et al., 2015*) and 10 minutes by a regional level system established by the Pacific Tsunami Warning Center (*PTWC, 2016*).

8. Output Image

The simulation outputs consisted of the maximum amplitude, maximum flow velocity, maximum hydrodynamic force and arrival time (for tsunami amplitudes higher than 0.05 m). A visualization of the results (maximum amplitude and arrival time) is shown below.

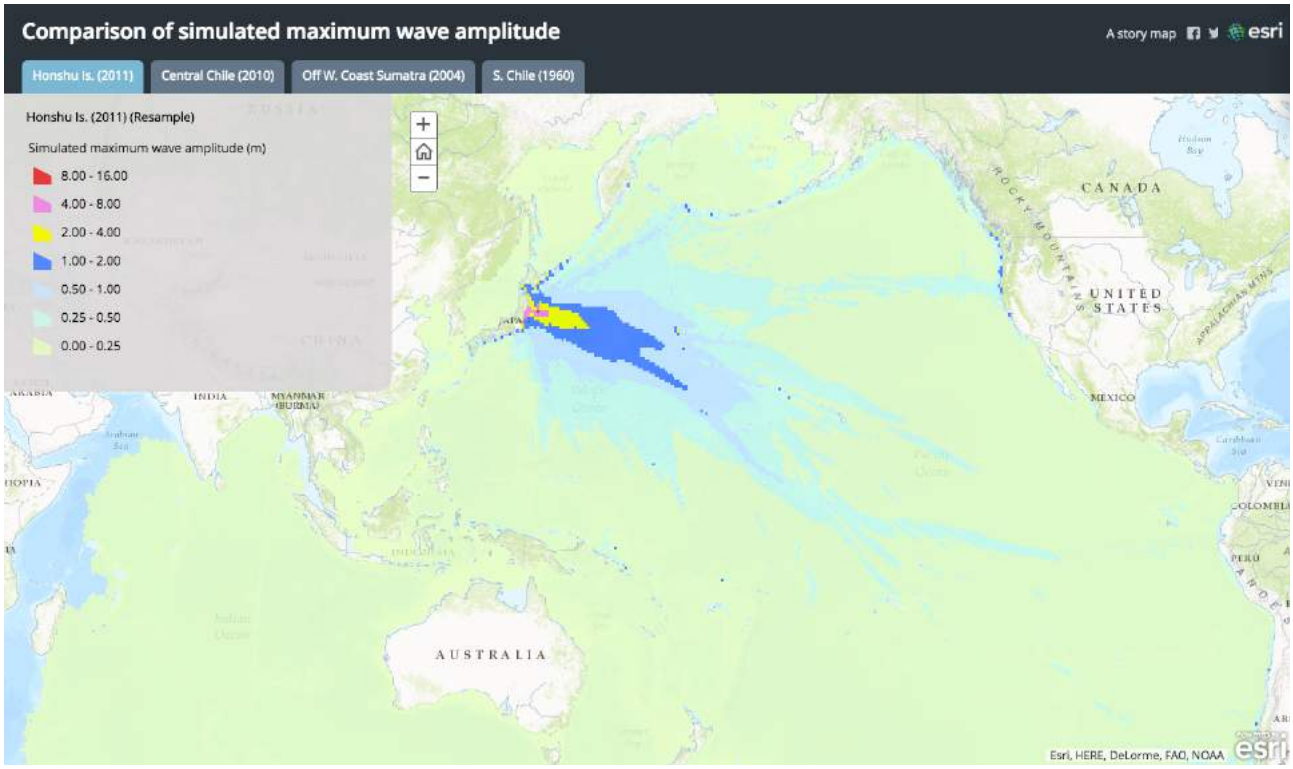

Figure 7

Maximum offshore tsunami amplitude distribution

***Note*. An example from the 2011 Great East Japan earthquake and tsunami)**

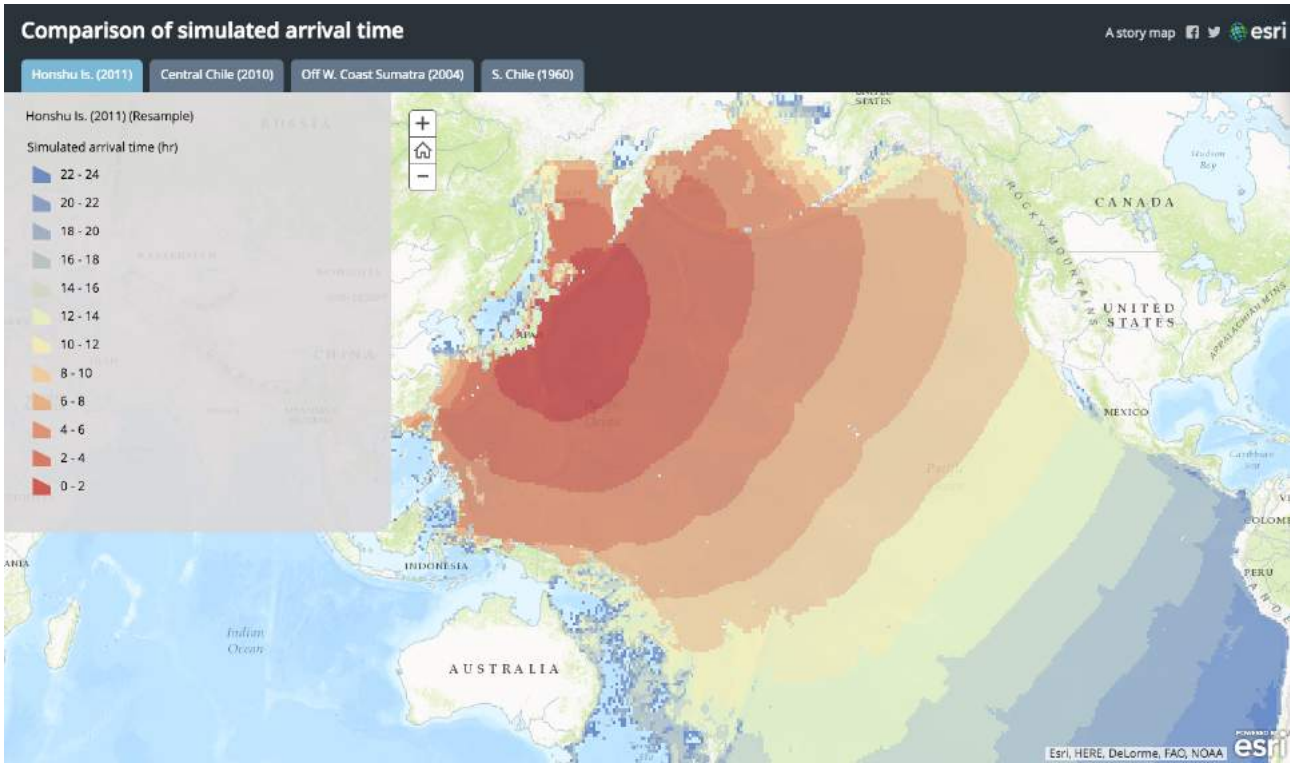

Figure 8

Tsunami arrival time

***Note*. An example from the 2011 Great East Japan earthquake and tsunami**

Q: A What are the factors that influence the arrival time of a tsunami?

A: The arrival time of tsunami depends on the distance from the tsunami source and sea depth. In the case of the 1993 Hokkaido Earthquake, the first tsunami arrived within 4-5 minutes after the earthquake as the epicenter was very close to the affected area (*National Oceanic and Atmospheric Administration (NOAA), 2016*). Tsunamis can travel as fast as an aircraft in the deep sea and at the speed of a vehicle in shallower areas. In case of the 2004 Indian Ocean Earthquake, the tsunami arrived at Thailand almost the same time as it arrived at Sri Lanka. This is because even though the distance from the earthquake to Thailand is shorter, the average sea depth to Thailand is much shallower (*Suppasri et al., 2016*).

9. Discussion

9.1 Gap between Historical and Recent Tsunamis

Memories and traditions of tsunami events can be limited and as a result a gap between our experiences and historical tsunamis continue to persist. **Figures 9** and **10** display the simulated maximum tsunami amplitude based on 34 and 52 events (excluding the events that affected the Atlantic Ocean) from the periods of 1970-2016 and 1600-1969, respectively. A tsunami amplitude of 2 m was selected as the criterion in this map because the damage from a tsunami significantly increases when the tsunami exceeds 2 m. **Figure 9** displays the locations of tsunamis that exceeded 2 m were mainly located in areas affected by the 2004 Indian Ocean Tsunami and the 2011 Great East Japan Tsunami based on recent experiences (1970-2016). On the other hand, damaging tsunamis that exceeded 2 m was seen virtually everywhere, especially along the Pacific Rim. **Figure 11** shows the results of the remaining seven events in Atlantic Ocean during 1600-1969 (it should be noted that there have been no events since 1969). It can be seen that southwest of Europe, northwest of Africa and areas neighboring Caribbean Sea were affected by tsunamis that exceeded 2 m. The one last event in this analysis is the 2013 Scotia Sea in the Southern Ocean near Antarctica which the simulated tsunami amplitude is too small to display, being under 2m.

This observation demonstrates the importance of assessing or recognizing the hazards based on historical events beyond recent experiences.

Figures 9 , **10** and **11** can also be interpreted by using a tsunami intensity scale that was proposed by *Papadopoulos and Imamura (2001)*. The tsunami intensity (*I*) scale (**Table 2**) (twelve grades) is independent of any physical parameters and includes the effects on humans and natural environments and the vulnerability of structures based on recent experiences regarding tsunamis. The tsunami intensity grades I–V refer to small tsunamis, where shaking from the earthquake could not be felt. Intensity grade VI indicates a slightly damaging tsunami. Intensity grades VII–VIII are used to define damaging and heavily damaging tsunamis, whereas grades IX–X refer to destructive and very destructive tsunamis. Finally, intensity grades XI–XII denote devastating and completely devastating tsunamis. The correlation of the maximum tsunami heights for each intensity grade is shown according to a power function of 2, which varies from zero to five (**Table 2**). The color bar of the maximum tsunami amplitude was also set following the tsunami intensity scale to improve visualization (*see* **Table 2**).

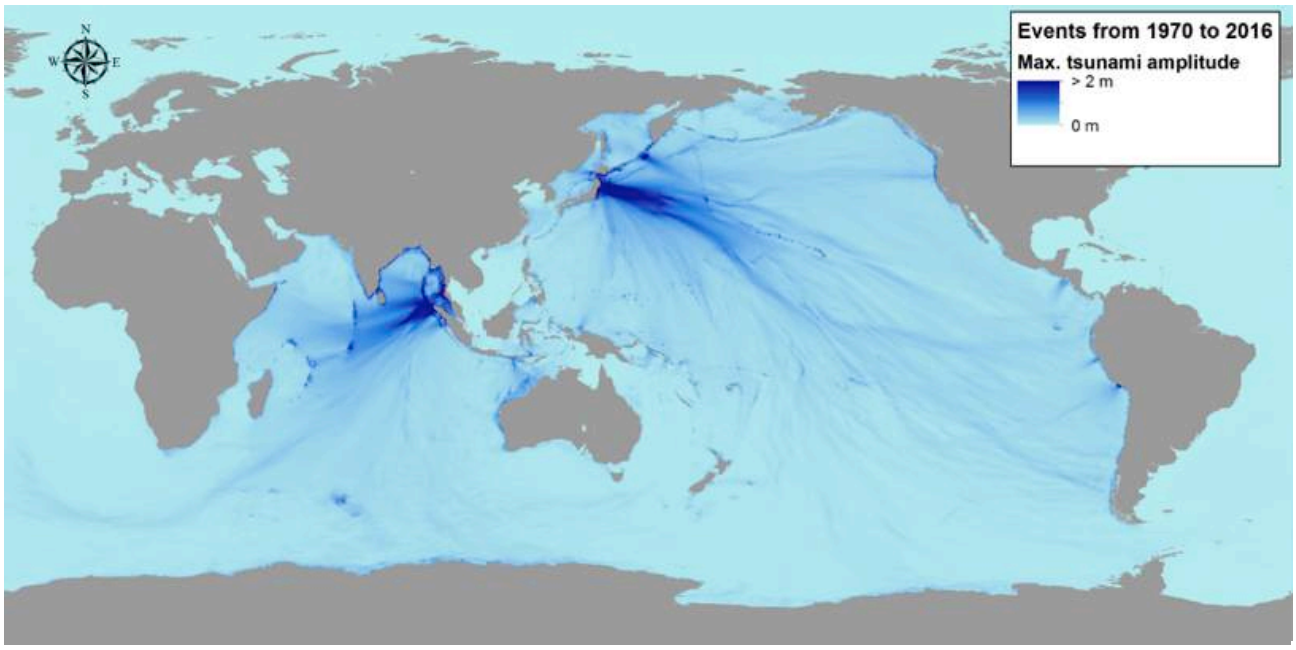

Figure 9

Simulated maximum tsunami amplitude based on events from 1970 to 2016 (Pacific and Indian Oceans)

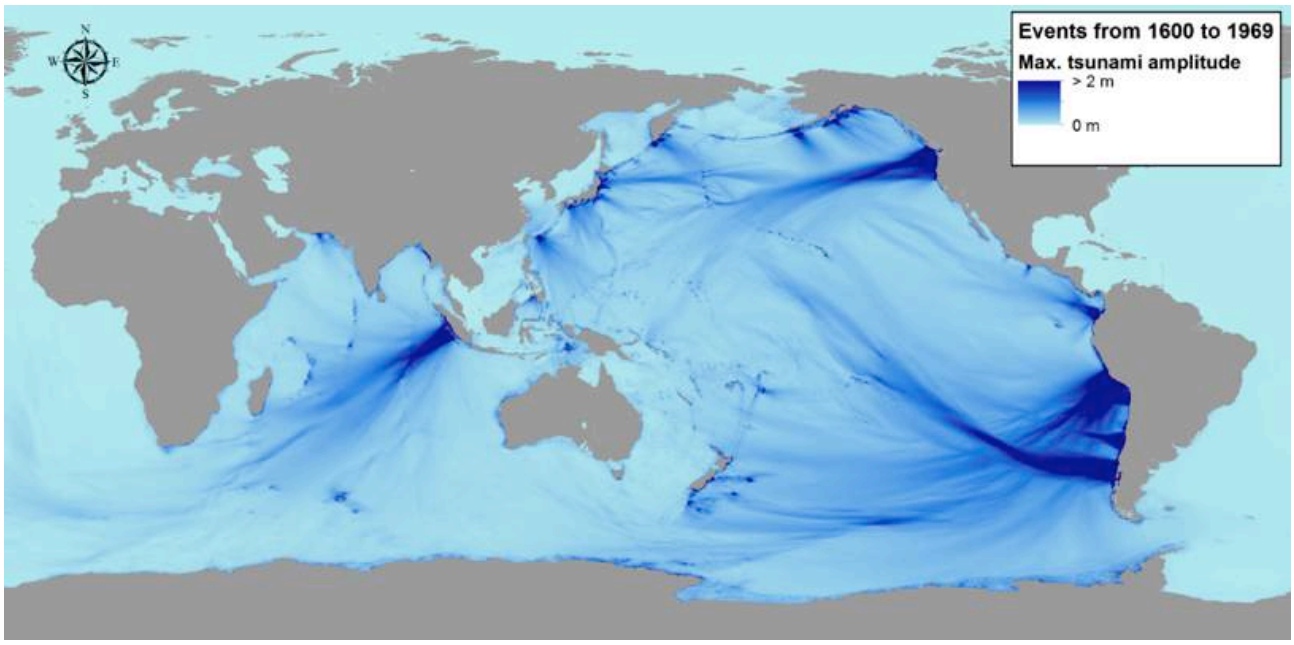

Figure 10

Simulated maximum tsunami amplitude based on events from 1600 to 1969 (Pacific and Indian Oceans)

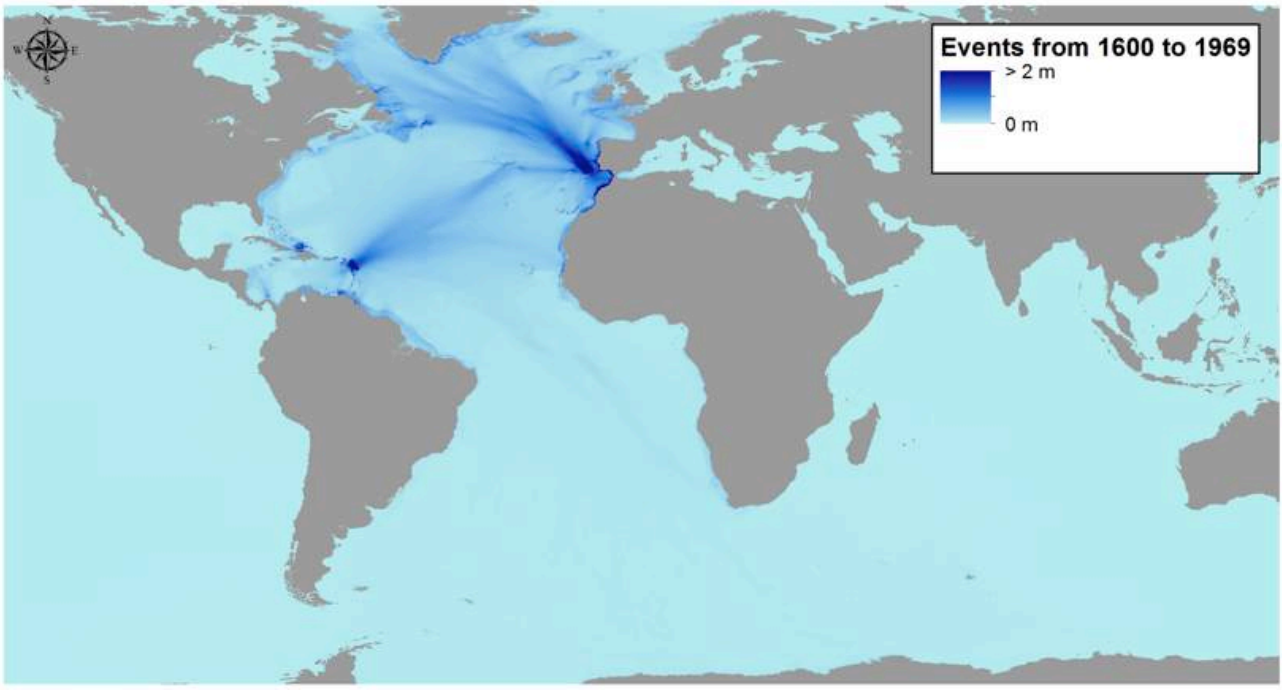

Figure 11

Simulated maximum tsunami amplitude based on events from 1600 to 1969 (Atlantic Ocean)

Q: How far inland can a tsunami travel?

A: Small tsunamis can be fully or partially mitigated by coastal defense structures such as breakwaters and seawalls. However, large tsunamis such as the ones generated by the 2004 Indian Ocean can penetrate as far as 1-2 km in Khao Lak, Thailand (*Suppasri et al., 2011*), 3-4 km in Banda Aceh, Indonesia (*Suppasri et al., 2015*), as well as 4-5 km in the Sendai Plains in case of the 2011 Great East Japan tsunami (*Suppasri et al., 2012*).

Table 2 **Tsunami intensity and correlated maximum shoreline tsunami amplitude**

Intensity (*I*)	Definition	Max. Shoreline Amplitude	Color Bar
I–V	Not felt (I), Scarcely felt (II), Weak (III), Largely observed (IV) and Strong (IV)	< 1.00 m	0.00 - 0.25 m 0.25 - 0.50 m 0.50 - 1.00 m
VI	Slightly damaging (VI)	< 2.00 m	1.00 - 2.00 m
VII–VIII	Damaging (VII) and Heavily damaging (VIII)	< 4.00 m	2.00 - 4.00 m
IX–X	Destructive (IX) and Very destructive (X)	< 8.00 m	4.00 - 8.00 m
XI–XII	Devastating (XI) and Completely devastating (XII)	> 8.00 m	> 8.00 m

9.2 Differences between Tsunami Height and Wave Force

Tsunami height is a typical hazard index applied to tsunamis and the most frequently used to understand the characteristics of a tsunami and damage. Wave force was selected as the most suitable factor to explain the risk according to recent data of damaged houses, boats and infrastructures. Some examples from two regions are shown to understand the differences between tsunami height and wave force.

The wave force as hydrodynamic force is often calculated by using the drag equation (drag force, F_D), as shown in **equation (4)** below.

$$F_D = 0.5 \times C_d \times \rho \times A \times U^2 \quad (4)$$

where F_D represents drag force, which is defined as the force component in the direction of the flow velocity; C_d is the drag coefficient (= 2.0 for a rectangular box); ρ is the mass density of the fluid (= 1,000 km/m^3 for water); A is the reference area (= tsunami height × building width); and U is the flow velocity relative to the object. This simulation calculated the drag force per meter as the building unit width. Therefore, the unit of the drag force is kN/m.

Table 3 demonstrates the relationship between building damage and the required tsunami height and hydrodynamic force based on building damage data from Japan.

Table 3 Relationship between building damage and required tsunami height and hydrodynamic force

Building Composition	Moderate Damage	Major Damage
Wood	1.5 m / 15.6 - 27.4 kN/m	2.0 m / 27.4 - 49.0 kN/m
Reinforced Concrete (RC)	N/A / 61 - 111 kN/m	8.0 m / 332 - 603 kN/m

Figure 12 displays an example of the importance of using the hydrodynamic force to assess building damage. The 2011 Great East Japan Tsunami was selected as a representative large tsunami event that caused damage over a wide area. This section focuses on damage to RC buildings by using major damage criteria of 7 m and 300 kN/m. The simulated maximum tsunami height was clearly higher than 7 m along the Sanriku Ria coast and lower than 7 m along the Sendai Plains coast (Region A). Nevertheless, the maximum simulated hydrodynamic force (higher than 300 kN/m) was found along the shoreline of both areas including Region A where decreased in Region B. Thus, only utilizing only tsunami height could underestimate the degree of building damages.

Figures 13 and **14** show another example with the 1852 Banda Sea Tsunami as a representative of a small tsunami inside a small sea that is surrounded by many small islands. At the deepest part of the bay, the maximum simulated tsunami height and hydrodynamic force were 4.93 m and 77.6 kN/m, respectively. However, the maximum hydrodynamic force (121.15 kN/m) was located at the edge of the bay, where the tsunami height was only 2.69 m. In addition, the tsunami height at the bay entrance was only 1.59 m but the hydrodynamic force was 62.57 kN/m. Thus, wooden houses might be interpreted as having experienced moderate damage when using the tsunami height or major/ complete damage when using the hydrodynamic force.

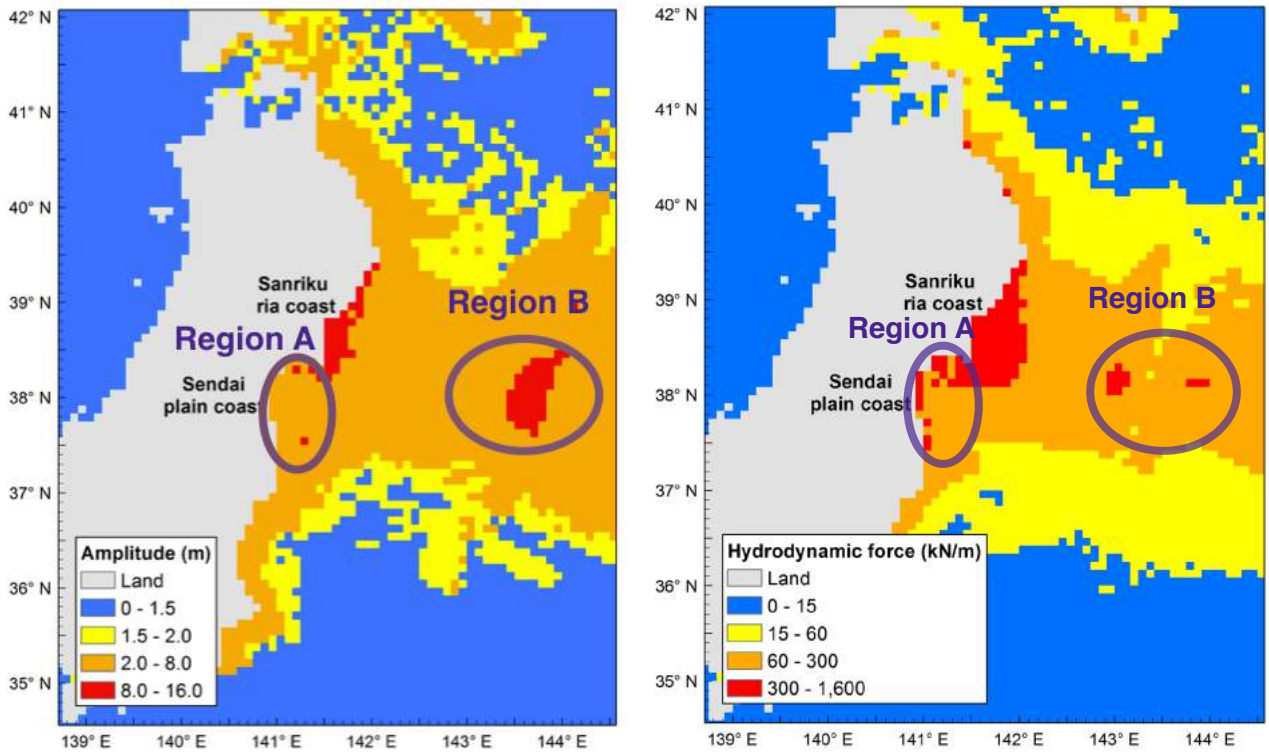

Figure 12

Simulated maximum tsunami height in meters (left) and hydrodynamic force in kN/m (right) for the 2011 Great East Japan tsunami

***Note*. Higher risk of building damage can be seen in region A when considering the hydrodynamic forces.**

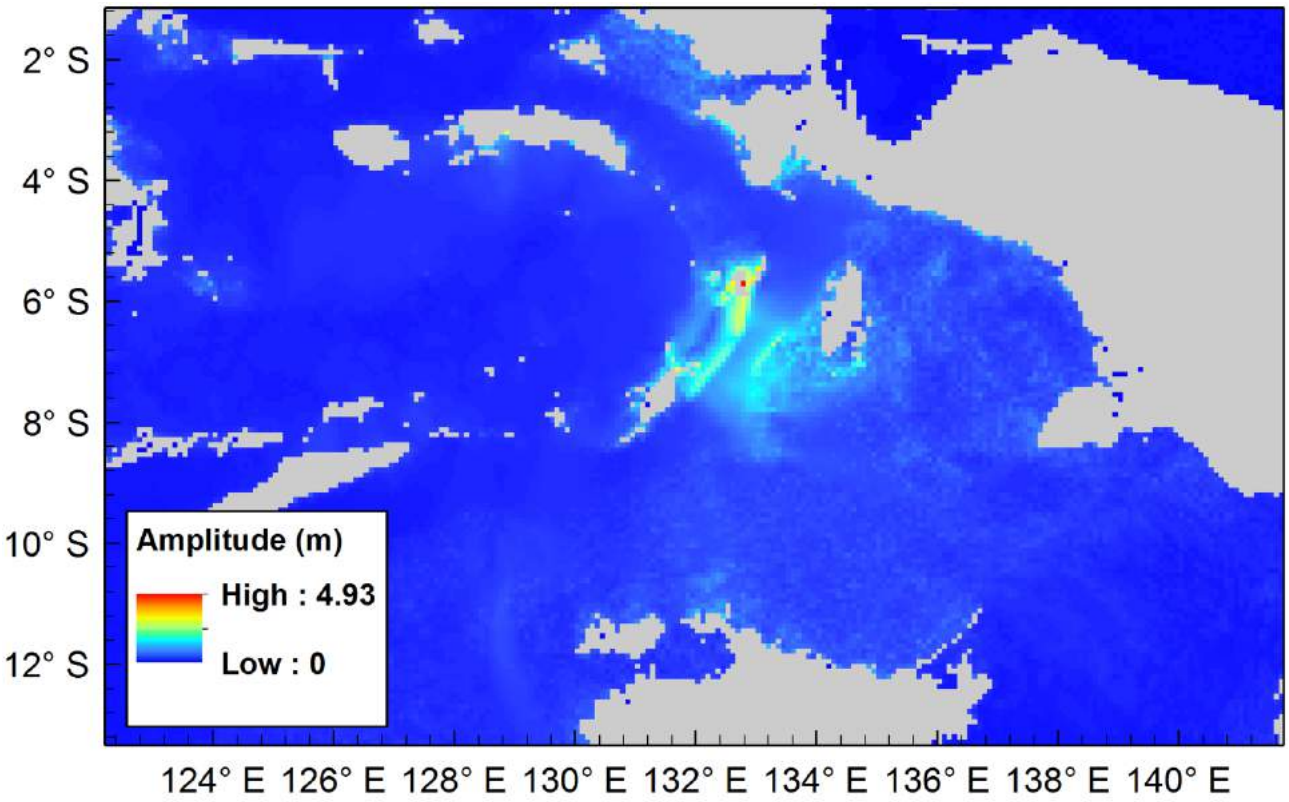

Figure 13

Simulated maximum tsunami height in meters (left) and hydrodynamic force in kN/m (right) for the 1852 Banda Sea tsunami (regional scale)

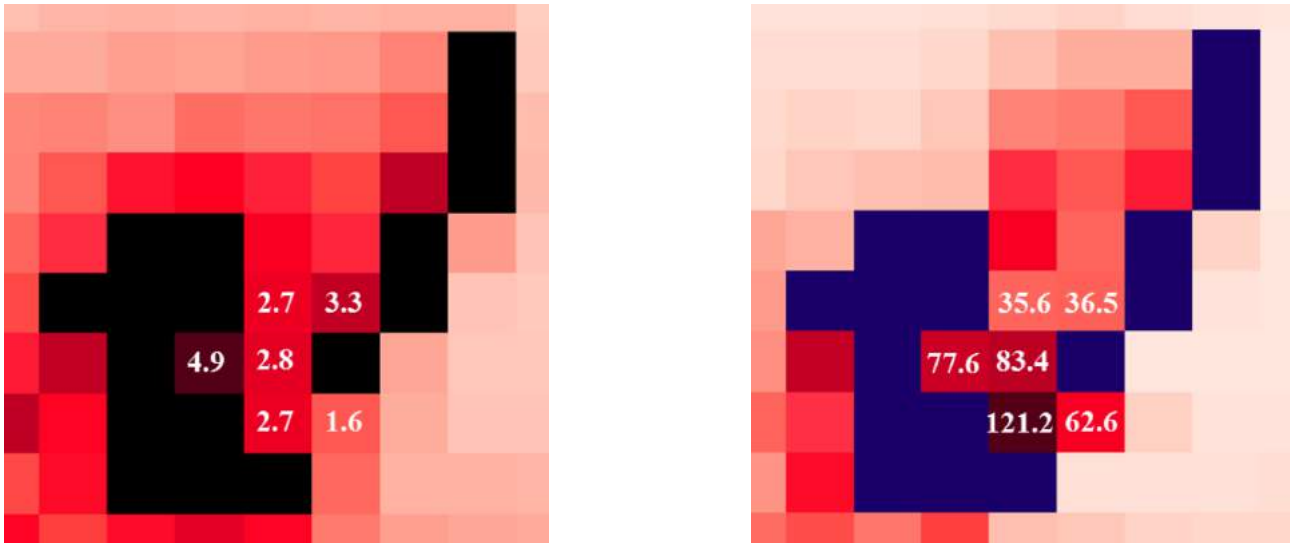

Figure 14

Simulated maximum tsunami height in meters (left) and hydrodynamic force in kN/m (right) for the 1852 Banda Sea tsunami (local scale near the tsunami source)

9.3 Tsunami Traveling Times

It is imperative to determine the arrival time of a tsunami in order to properly evacuate people located in at-risk areas. Arrival time is estimated from source location, topography and bathymetry, and its influence on the speed of the waves. **Figure 15** displays tsunami propagation and the travel time of the 2004 Indian Ocean tsunami.

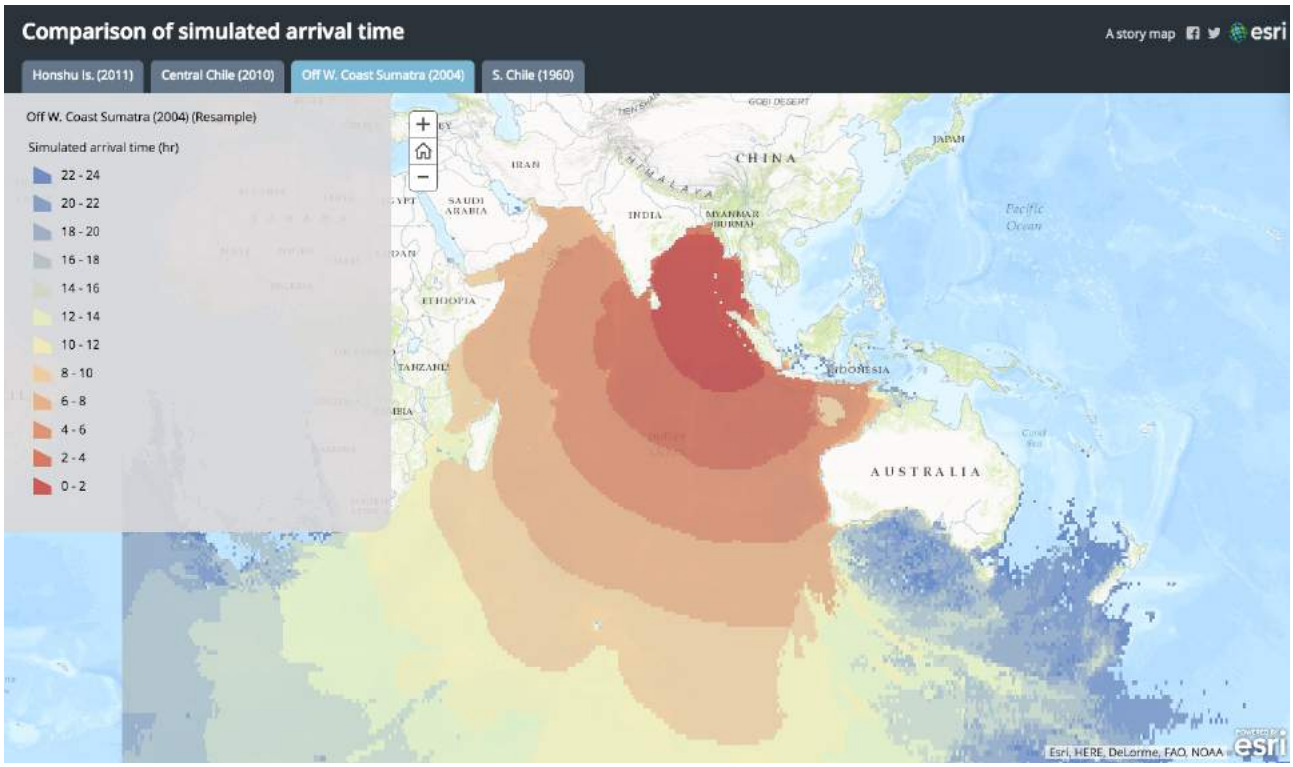

Figure 15

Tsunami arrival time

***Note*. An example from the 2004 Indian Ocean tsunami**

10. Conclusions

- A global tsunami assessment has been developed based on select 100 major historical earthquake-generated tsunamis

- This observation demonstrates the importance of assessing or understanding the hazards based on historical events beyond recent experiences

- Comparisons between tsunami height and wave force demonstrate that only using the tsunami height might underestimate the extent of building damage

- Potential events such as events in seismic gap as well as other types of tsunami sources should be added for assessing future hazards

- This report can contribute as supplementary information for policy makers, urban planners, engineers, as well as scholarly research

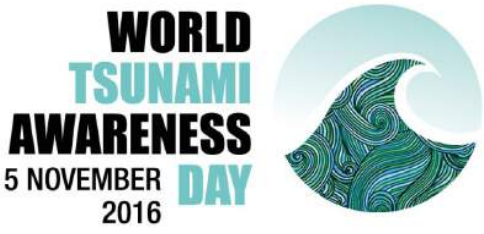

"We wish that as a part of the World Tsunami Awareness Day related activities, our results and findings will increase tsunami awareness at the global scale especially in comparatively low tsunami risk areas, and reduce human loss from tsunamis in the future."

11. References

Atwater, B. F., Musumi-Rokkaku, S., Satake, K., Tsuji, Y., Ueda, K., & Yamaguchi, D. K. (2015). *The orphan tsunami of 1700-Japanese clues to a parent earthquake in North America* (2nd ed.). Seattle, University of Washington Press, U.S. Geological Survey Professional Paper 1707.

Dziewonski, A. M., Chou, T. A., & Woodhouse, J. H. (1981). Determination of earthquake source parameters from waveform data for studies of global and regional seismicity. *Journal of Geophysical Research: Solid Earth, 86*(B4), 2825-2852. doi: 10.1029/JB086iB04p02825

Fujii, Y., & Satake, K. (2013). Slip distribution and seismic moment of the 2010 and 1960 Chilean earthquakes inferred from tsunami waveforms and coastal geodetic data. *Pure and Applied Geophysics, 170*(9), 1493-1509. doi: 10.1007/s00024-012-0524-2

General Bathymetric Chart of the Oceans (GEBCO) (2016). *Gridded bathymetry data*. Retrieved Aug. 6, 2016, from http://www.gebco.net/data_and_products/gridded_bathymetry_data

Ichinose, G., Somerville, P., Thio, H. K., Graves, R., & O'Connell, D. (2007). Rupture process of the 1964 Prince William Sound, Alaska, earthquake from the combined inversion of seismic, tsunami, and geodetic data. *Journal of Geophysical Research, 112*(B7), B07306. doi: 10.1029/2006JB004728

Imamura, F. (1996). Simulation of wave-packet propagation along sloping beach by TUNAMI-code. In H. Yeh, P. Liu, & C. Synolakis (Eds.), *Long-wave Sunup Models* (pp. 231-241), Singapore: World Scientific.

Imamura, F., Yalciner, A. C., & Ozyurt, G. (2006). *Tsunami Modelling Manual (TUNAMI model)*. Miyagi: Tsunami Engineering Laboratory, Tohoku University.

IUGG/IOC TIME Project. (1997). IUGG/IOC TIME Project: Numerical method of tsunami simulation with the leap-frog scheme. *Intergovernmental Oceanographic Commission Manuals and Guides, 35*. Geneva: UNESCO.

Johnson, J. M., & Satake, K. (1999). Asperity distribution of the 1952 Great Kamchatka earthquake and its relation to future earthquake potential in Kamchatka. *Pure and Applied Geophysics, 154*(3), 541-553. doi: 10.1007/s000240050243

Leelawat, N., Suppasri, A., & Imamura, F. (2015). The tsunami warning system in Thailand: A part of the reconstruction process after the 2004 Indian Ocean Tsunami. In V. Santiago-Fandiño, Y. A. Kontar, & Y. Kaneda (Eds.), *Advances in Natural and Technological Hazards Research: Vol. 44. Post-Tsunami Hazard: Reconstruction and Restoration* (pp. 111-119), Cham: Springer International Publishing. doi: 10.1007/978-3-319-10202-3_8

Løvholt, F., Glimsdal, S., Harbitz, C. B., Zamora, N., Nadim, F., Peduzzi, P., Dao, H., & Smebye, H. (2012). Tsunami hazard and exposure on the global scale. *Earth-Science Reviews 110*(1), 58-73. doi: 10.1016/j.earscirev.2011.10.002

Nagano, O., Imamura, F., & Shuto, N. (1991). A numerical model for a far-field tsunamis and its application to predict damages done to aquaculture. *Natural Hazards 4*(2). 235-255. doi: 10.1007/BF00162790

National Geophysical Data Center / World Data Service (NGDC/WDS). (2015). *Global Historical Tsunami Database*. National Geophysical Data Center, NOAA. Retrieved Sep. 21, 2016, from doi: 10.7289/V5PN93H7

National Oceanic and Atmospheric Administration (NOAA). (2016). *Hokkaido Nansei-Oki Tsunami, July 12, 1993*. Retrieved October 27, 2016, from https://catalog.data.gov/dataset/hokkaido-nansei-oki-tsunami-july-12-1993

Okada, Y. (1985). Surface deformation due to shear and tensile faults in a half-space. *Bulletin of the Seismological Society of America, 75*(4), 1135-1154.

Okal, E. A., Synolakis, C. E., Uslu, B., Kalligeris, N. and Voukouvalas, E. (2009) The 1956 earthquake and tsunami in

Amorgos, Greece, *Geophysical Journal International. 178*(3), 1533-1554. doi: 10.1111/j.1365-246X. 2009.04237.x

Papadopoulos G. A., & Imamura, F. (2001). A proposal for a new tsunami intensity scale. *Proceedings of the International Tsunami Symposium, Session: 5, No. 5-1* (pp. 569-577), Seattle, WA.

Papazachos B. C., Scordilis, E. M., Panagiotopoulos, D. G., Papazachos, C. B., & Karakaisis, G. F. (2004). Global relations between seismic fault parameters and moment magnitude of earthquakes. In *Bulletin of the Geological Society of Greece, Vol: 36, No: 3, Proceedings of the 10th International Congress* (pp. 1482-1489), Thessaloniki, Greek.

Pacific Tsunami Warning Center. (2016). *Frequently Asked Questions (FAQ)*. Retrieved October 27, 2016, from http://www.tsunami-alarm-system.com/en/phenomenon-tsunami/occurrences-atlantic-ocean.html

Piatanesei, A., & Tinti, S. (2002). Numerical modelling of the September 8, 1905 Calabrian (southern Italy) tsunami. *Geophysical Journal International, 150*(1), 271-284. doi: 10.1046/j.1365-246X. 2002.01700.x

Santos, A., Koshimura, S., & Imamura, F. (2009). The 1755 Lisbon tsunami: Tsunami source determination and its validation. *Journal of Disaster Research, 4*(1), 41-52. doi: 10.20965/jdr. 2009.p0041

Suppasri, A., Imamura, F., & Koshimura, S. (2010). Effects of the rupture velocity of fault motion, ocean current and initial sea level on the transoceanic propagation of tsunami. *Coastal Engineering Journal, 52*(2), 107-132. doi: 10.1142/S0578563410002142

Suppasri, A., Koshimura, S., & Imamura, F. (2011). Developing tsunami fragility curves based on the satellite remote sensing and the numerical modeling of the 2004 Indian Ocean tsunami in Thailand. *Natural Hazards and Earth System Sciences, 11*(1), 173-189. doi: 10.5194/nhess-11-173-2011

Suppasri, A., Koshimura, S., Imai, K., Mas, E., Gokon, H., Muhari, A., & Imamura, F. (2012). Damage characteristic and field survey of the 2011 Great East Japan tsunami in Miyagi prefecture. *Coastal Engineering Journal, 54*(1), 1250008. doi: 10.1142/S0578563412500052

Suppasri, A., Goto, K., Muhari, A., Ranasinghe, P., Riyaz, M., Affan, M., Mas, E., Yasuda, M., & Imamura, F. (2015). A decade after the 2004 Indian Ocean tsunami- The progress in disaster preparedness and future challenges in Indonesia, Sri Lanka, Thailand and the Maldives. *Pure and Applied Geophysics, 172*(12), 3313-3341. doi: 10.1007/s00024-015-1134-6

Suppasri, A., Latcharote, P., Bricker, J. D., Leelawat, N., Hayashi, A., Yamashita, K., Makinoshima, F., Roeber, V., & Imamura, F. (2016). Improvement of tsunami countermeasures based on lessons from the 2011 great east japan earthquake and tsunami -Situation after five years-. *Coastal Engineering Journal, 58*(4), 1640011. doi: 10.1142/S0578563416400118

Tsunami Alarm System. (2016a). *Occurrences of Tsunamis in the Atlantic Ocean*. Retrieved October 27, 2016, from http://www.tsunami-alarm-system.com/en/phenomenon-tsunami/occurrences-atlantic-ocean.html

Tsunami Alarm System. (2016b). *Occurrences of Tsunamis in the Mediterranean*. Retrieved October 27, 2016, from http://www.tsunami-alarm-system.com/en/phenomenon-tsunami/occurrences-mediterranean.html

Tsunami Laboratory. (2016). *Analysis of the Tsunami Travel Time maps for damaging tsunamis in the World Ocean*. Retrieved October 27, 2016, from http://tsun.sscc.ru/TTT_rep.htm

United Nations International Strategy for Disaster Reduction (UNISDR). (2009). *Global Assessment Report 2009, Risk and poverty in a changing climate, Invest today for a safer tomorrow*. Retrieved Oct. 13, 2016, from http://www.preventionweb.net/english/hyogo/gar/2009/?pid:34&pif:3

U.S. Geological Survey (USGS). (2016). *Earthquake Glossary - seismic gap*. Retrieved October 27, 2016, from http://www.tsunami-alarm-system.com/en/phenomenon-tsunami/occurrences-mediterranean.html

Wang, D., & Becker, N. (2015). *Tsunami forecast model animation of the 1 November 1755 Lisbon, Portugal tsunami*. Retrieved October 27, 2016, from https://www.youtube.com/watch?v=7DpF38OKYz0

Contact

IRIDeS, Tohoku University

email

Professor Dr. Fumihiko Imamura
imamura@irides.tohoku.ac.jp

Associate Professor Dr. Anawat Suppasri
suppasri@irides.tohoku.ac.jp

Dr. Panon Latcharote
panon@irides.tohoku.ac.jp

Mr. Takuro Otake
takuro.ohtake.q2@dc.tohoku.ac.jp

Postal Address

International Research Institute of Disaster Science (IRIDeS)
Tohoku University
468-1 Aramaki-Aza Aoba, Aoba-ku
Sendai 980-0845 Japan

Phone

+81-22-752-2092

Fax

+81-22-752-2091

URL

http://irides.tohoku.ac.jp/

Download the latest version of this report at
http://irides.tohoku.ac.jp/project/global_assessment_tsunami_hazards.html

Acknowledgments

We would like to express our deep gratitude to **Assistant Professor. Dr. Natt Leelawat** of IRIDeS, Tohoku University, for his support in creating the design and layout of this report and **David N. Nguyen** of Tohoku University, for his support this report's translation.

WORLD TSUNAMI AWARENESS DAY
5 NOVEMBER 2016